Contents lists available at SciOpen

Food Science and Human Wellness

journal homepage: https://www.sciopen.com/journal/2097-0765

China Food Publishing Co.

Effective detection of chloramphenicol residues by self-assembled DNA tetrahedral structure-based electrochemical aptasensor

Zihan Gao[a,b], Yu Zhou[a], Li Lin[a], Changyuan Yu[b], Hao Li[a,*]

[a] School of Public Health, Jining Medical University, Jining 272067, China
[b] College of Life Science and Technology, Beijing University of Chemical Technology, Beijing 100029, China

ARTICLE INFO

Article history:
Received 8 November 2023
Received in revised form 21 January 2024
Accepted 19 June 2024

Keywords:
Tetrahedral structure
Chloramphenicol
Electrochemical aptasensor
Milk

ABSTRACT

Abuse of chloramphenicol (CAP) could cause serious side effects to human health. Therefore, it is necessary to detect CAP residues in animal sourced food effectively. Here, the superiority (better stability, higher Apt-CAP loading efficiency, and higher CAP binding associated conformational change, etc.) of tetrahedral structure to double-chained structure for developing aptasensor was evaluated. Then, a self-assembled DNA tetrahedral structure-based electrochemical aptasensor targeting CAP was developed. Under the optimized conditions, the aptasensor exhibited high sensitivity toward CAP with a limit of detection (LOD) of 0.067 6 ng/mL (linear range 0.19−387.76 ng/mL), and high selectivity against the structural analogs of CAP. Moreover, the recovery rate of CAP from spiked milk samples ranged from 100.57% to 101.69%, and only USD 1.34 is needed for detecting CAP in 1 sample. These results suggested the application potential of this aptasesor for detecting CAP in animal sourced foods.

1. Introduction

Chloramphenicol (CAP), as a broad-spectrum antibiotic, is widely used in animal husbandry to prevent and treat diseases by inhibiting the activity of Gram-positive and negative bacteria[1]. However, excessive abuse is still present, and the residual CAP could be released into the environment and enter human body through food chain, finally causing food safety problems and posing a huge threat to public health[2]. Due to its serious side effects, under the recommendation of the Joint Food and Agriculture Organization/World Health Organization (FAO/WHO) Expert Committee on Food Additives (JECFA)[3], including the European Union (EU) and other regulatory agencies around the world established a maximum residue limit (MRL) for CAP. Among them, the EU sets the MRL of CAP in milk, meat, aquatic products and other foods as 0.3 μg/kg[4], while China has clearly banned the use of CAP in poultry, livestock and animal-sourced foods. Therefore, it is necessary to carry out efficient quantitative detection of CAP content in animal-sourced food.

Currently, the most popular methods for detection of CAP residues mainly include gas chromatography (GC)[5], high-performance liquid chromatography-tandem mass spectrometry (HPLC-MS)[6], and enzyme-linked immunosorbent assay (ELISA)[7]. However, these reported methods generally have the drawbacks of long detection time, high detection cost, and high requirements for equipment and professional operators[8]. Therefore, it is necessary to establish an alternative method for sensitively and specifically identifying CAP.

Aptamers refer to single-stranded DNA or RNA fragments with a length of 20−100 bp[9], and their high recognition and binding activity towards targets[10], easy modification, and high stability

* Corresponding author at: School of Public Health, Jining Medical University, Jining 272067, China.
E-mail address: lihao@mail.jnmc.edu.cn (H. Li)
Peer review under responsibility of Beijing Academy of Food Sciences.

SciOpen Publishing services by Tsinghua University Press

http://doi.org/10.26599/FSHW.2024.9250341

make aptamers suitable for constructing biosensor platforms. Due to these advantages, aptamers have been widely used as biorecognition elements to develop biosensors for detection of drug residues[11-12], environmental pollutants[13], and diagnostic markers[14]. For example, aptamer-based sensors have been fabricated for detecting CAP to guarantee food safety[15-16]. Moreover, our previous work also reported an aptasensor, enabling simultaneous detection of CAP and kanamycin[17]. However, the common double-chained structure traditionally used for aptasensor construction has disadvantages of few binding sites and low stability over a long period of time, so an aptasensor based on tetrahedral structure was constructed in this study.

The DNA tetrahedral structure, first being proposed in 2004, is the most classic nanostructure[18]. Since its each surface is a complete triangle, the tetrahedron has excellent structural stability and controllability. Meanwhile, the unique characteristics of tetrahedral structure, such as simple synthesis and size homogeneity[19], make it widely used as a superior DNA nanomaterial in various fields, including biosensors. For example, a label-free electrochemical sensor based on DNA nanostructure was developed for the detection of miR-155[20]; and a novel electrochemiluminescence aptasensor based on Au-tetrahedral aptamer nanostructure was also fabricated for acetamiprid detection[21]. Here, tetrahedral structure would also provide more binding sites for aptamers to improve the loading capacity of specific aptamers, thereby promoting the detection performance.

In this study, the superiority of tetrahedral structure to double-chained structure for developing aptasensor was evaluated by comparing respective aptamer (i.e., Apt-CAP) loading capacity, structure stability and CAP binding associated conformational change (i.e., analyzed through circular dichroism analysis). Then a tetrahedral structure-based electrochemical aptasensor targeting CAP was developed. Upon the addition of CAP, its aptamer would specifically bind with CAP and be released from the tetrahedral structure, thereby leading to release of the electroactive substance methylene blue (MB). Therefore, the quantitative detection of CAP can be achieved by monitoring the electrochemical signal change on the electrode surface. While achieving sensitive detection, the tetrahedral structure-based aptasensor effectively improved the Apt-CAP loading capacity, placement stability and reusability of specific aptamers on the electrode surface, and showed great potential for CAP detection in actual milk samples. Meanwhile, the lower detection cost also makes this aptasensor to be a more efficient and economical method for CAP detection.

2. Materials and methods

2.1 Chemicals and reagents

DNA oligonucleotide sequences were synthesized and purified by HPLC or hPAGE by GENEWIZ Co. (Suzhou, China) and listed in Table S1. The aptamer Apt-CAP specifically against CAP with K_d value of 0.766 μmol/L was reported by Mehta et al.[22]. Concentrated sulfuric acid and chloroauric acid ($HAuCl_4 \cdot 4H_2O$, Au) were purchased from Sinopharm Chemical Reagent Co., Ltd. (Shanghai, China). CAP, potassium ferricyanide, 6-mercapto-1-hexanol (MCH), MB, $MgCl_2 \cdot 6H_2O$, glacial acetic acid, disodium EDTA-2Na, boric acid, acrylamide, *N*,*N*,*N*',*N*'-tetramethylethylenediamine (TEMED), and ammonium persulfate (APS) were purchased from Shanghai McLean Biochemical Technology Co., Ltd. (Shanghai, China). PBS buffer and Tris were purchased from Beijing Solarbio Technology Co., Ltd. (Beijing, China). Graphene oxide TNGO-3 was purchased from Chengdu Zhongke Times Nano Energy (Chengdu, China). Tris (2-carboxyethyl) phosphine hydrochloride (TCEP) was purchased from Shanghai Yuanye Biotechnology Co., Ltd. (Shanghai, China). DPBS buffer was purchased from Wuhan Proceeds Life Technology Co., Ltd. (Wuhan, China). All the reagents and chemicals were of analytical grade and could be used without further purification. Aqueous solutions were prepared with deionized water (Simple-Q15 system, Zhi Ang, resistance 17.5 MΩ·cm) throughout the experiments.

2.2 Synthesis and characterization of tetrahedral structure

Before preparing the DNA tetrahedral structure, the thiol-modified sequences S2, S3 and S4 were incubated with 1 mol/L TCEP solution at 4 ℃ for 1 h to reduce disulfide bonds. Afterwards, 4 sequences (S1, S2, S3 and S4) of equivalent amount of substance with a final concentration of 2×10^{-6} mol/L were dissolved in TM buffer (20×10^{-3} mol/L Tris, 12.5×10^{-3} mol/L $MgCl_2$, pH 8.0) before being heated at 95 ℃ for 10 min and cooled at 4 ℃ for 30 min. The DNA tetrahedral framework structure was verified by 8% native PAGE.

2.3 Evaluation of the potential of tetrahedral structure for developing aptasensor

The 3 chains (S2, S3, and S4 sequences) that flank the tetrahedral structure all contain base sequences that can complement the aptamer Apt-CAP; in other words, any of these 3 chains can be used to form complementary double strands with Apt-CAP. Here, the S3 sequence was selected to form a double-chained structure with Apt-CAP to evaluate the potential superiority of the tetrahedral structure to traditional double-chained structure for developing aptasensor. The Apt-CAP loading efficiency by these 2 different structures (tetrahedral structure and double-chained structure) was calculated. Circular dichroism (CD) analysis was performed to characterize the conformational changes of these 2 structures loaded with Apt-CAP (tetrahedron-aptamer complex and double-chained structure) over placement time lasting, as well as the difference in detection performance (represented by the CAP binding associated conformational changes). Apt-CAP was mixed with the DNA tetrahedral structure in a molar ratio of 3:1 before being heated at 95 ℃ for 10 min and cooled at 4 ℃ for 30 min to form the tetrahedron-aptamer complex. CD analysis was performed using a JASCO J-815 CD spectrometer (Tokyo, Japan). Each CD spectrum was collected at 1 nm intervals from 220 to 320 nm and data were an accumulation of 3 scans of 0.50 nm band width.

2.4 Preparation of the AuNPs/rGO modified electrode

The glassy carbon electrode with the diameter of 3 mm was sequentially polished by alumina powder with the diameters of 0.05 and 0.30 μm on polishing cloth in prior to ultrasonic clean in ethanol solution and ultrapure water for 3 min to remove residual Al_2O_3. The electrode was electrochemically cleaned by cyclic voltammetry (CV) scanning for 20 cycles with 0.5 mol/L H_2SO_4 as the electrolytic solution in the potential scanning from −1 to 1 V. After the electrode was cleaned with deionized water and naturally

dried, 4 μL of 1 mg/mL graphene oxide suspension was dropped onto the surface of the polished glassy carbon electrode. After natural drying, a constant voltage of −1.4 V was applied to the graphene oxide modified electrode in 0.1 mol/L PBS solution for 600 s to obtain electrochemically reduced graphene oxide (rGO). The modified electrode was placed in 10 mmol/L $HAuCl_4$ solution containing 0.5 mol/L H_2SO_4, and reduced at a constant potential of −0.2 V for 120 s to obtain the AuNPs/rGO modified electrode.

2.5 Establishment and optimization of the DNA tetrahedral structure-based electrochemical aptasensor

The tetrahedron-aptamer complex was formed according to the procedure described in Section 2.3. A total of 10 mL of the formed complex was dropped onto the surface of the pre-prepared AuNPs/rGO modified electrode and incubated at ice bath in dark to form Au-S bonds. After washing with deionized water, 10 L of 10 mmol/L MCH solution was dropped onto the surface of the electrode before incubation for 1 h to block the uncovered electrode surface sites, such operation was performed twice. Upon the addition of CAP, its binding with Apt-CAP would cause the conformational change of the latter to release the electroactive substance MB, thereby leading to the electrochemical signal change. The electrochemical signal of the MB was measured using square wave voltammetry (SWV) pattern in DPBS buffer by CHI 630E electrochemical workstation (Shanghai Chenhua Instrument Co., Ltd., Shanghai, China). A conventional three-electrode system was used with glassy carbon electrode as the working electrode, a platinum wire electrode as the counter electrode, and an Ag/AgCl (saturated KCl) electrode as the reference electrode.

The detection performance of the constructed aptasensor would be affected by the tetrahedron-aptamer complex concentration, the incubation time of the tetrahedron-aptamer complex with the electrode, and reaction time of the aptasensor with the target CAP. Therefore, these factors were further needed to be optimized.

2.6 Determination of the sensitivity and specificity of the electrochemical aptasensor

To determine the sensitivity of the developed aptasensor, various concentrations of CAP (from 0.6 nmol/L to 1.2 μmol/L) were respectively used. Meanwhile, the ultrapure water was utilized as the negative control. Under the optimized condition, CAP addition associated change of peak current value (ΔμA) was determined, and the lower limit of detection (LOD) of this aptasensor was calculated from the standard deviation (SD) and slope (K) of the standard curve with a signal-to-noise ratio of 3:1[23]. Moreover, the selectivity of the constructed aptasensor was evaluated using CAP and its structural analogs (thiamphenicol, florfenicol and streptomycin). Furthermore, the reusability and detection stability of the developed aptasensor were evaluated using CAP (120 nmol/L). For reusability evaluation, the electrode surface was thoroughly washed with deionized water after the previous detection to ensure the accuracy of the next detection. For detection stability evaluation, the electrochemical aptasensors prepared from five different batches were adopted to detect the same concentration of CAP (120 nmol/L).

2.7 Determination of CAP in actual spiked milk samples

CAP-free milk was purchased from the local supermarket and spiked to different final concentrations (5, 10 and 15 ng/mL) of CAP. Quantification of CAP in spiked milk samples was performed by the established aptasensor. The recovery rate (y) was calculated according to the following equation:

$$y\ (\%) = \frac{x_1}{x} \times 100 \quad (1)$$

In this equation, y (%) refers to the recovery rate; x_1 represents the measured CAP amount; x refers to the amount of CAP added initially.

2.8 Statistical analysis

Experimental data were expressed as the mean ± SD of 3 independent replicate experiments, and analyzed by using IBM SPSS statistics 22.0 (IBM Corp. Armonk, NY, USA).

3. Results and discussion

3.1 Synthesis and characterization of the tetrahedral structure

The tetrahedral structure consists of 4 single chains (S1, S2, S3, and S4). After thermal denaturation of single chain (S1), 2 chains (S1 and S2), 3 chains (S1, S2 and S3) and 4 chains (S1, S2, S3 and S4), the stepwise assembly process was characterized by gel electrophoresis (Fig. 1). Electrophoresis result indicated that the migration rates of these 4 chains were in a molecular weight (MW) dependent manner (Fig. 1), suggesting the gradually increased MW with the stepwise assembly process. Four chains in lane 4 with the slowest migration rate indicated the successful synthesis of the tetrahedral structure.

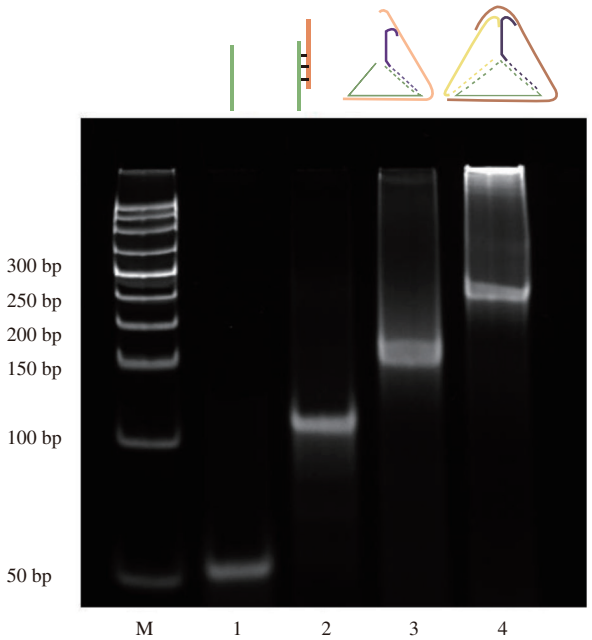

Fig. 1 Assembly process of the tetrahedral structure. M, marker; lane 1, single chain (S1); lane 2, 2 chains (S1 and S2); lane 3, 3 chains (S1, S2 and S3); lane 4, 4 chains (S1, S2, S3 and S4).

3.2 Superiority of tetrahedral structure over double-chained structure for developing aptasensor

CD spectroscopy analysis was used to elucidate the placement stability of these 2 structures loaded with Apt-CAP (tetrahedron-aptamer complex and double-chained structure) and the conformational changes upon CAP binding. Compared with that of the tetrahedron-aptamer complex structure (Fig. 2A), the CD spectral signal of the double-chained structure (Fig. 2B) exhibited more drastic conformational changes at 225, 240, 270 and 280 nm as placement time lasting, indicating higher stability of the tetrahedra based structure than that of the double-chained structure. Moreover, addition of CAP caused more obvious conformational change (a significant slope change between 260–290 nm) of the tetrahedral based structure (Fig. 2C) than that of the double-chained structure (Fig. 2D). The larger target binding associated CD spectral signal change usually suggests higher detection sensitivity of the fabricated aptasensor[24]. Here, both higher placement stability and CAP binding-associated conformational change would contribute to the high potential of the tetrahedral-based structure for developing an aptasensor.

Moreover, the Apt-CAP loading efficiency by these 2 different structures was calculated. The Apt-CAP loading of the tetrahedral structure was 7.49 μmol/L, which was approximately 3.5 times of that of the double-chained structure (Fig. 2E). The result indicated that under the same condition, the tetrahedral structure can combine more Apt-CAP, which was more beneficial to the detection sensitivity.

3.3 Principle of the developed electrochemical aptasensor

The detection performance of the aptasensor depends on the specific competition of CAP with the side chains (S2, S3 and S4 sequences) of the tetrahedral structure for the limited Apt-CAP (Fig. 3). The CAP detection system is immobilized on the surface of the modified glassy carbon electrode through Au-S bonds, and Apt-CAP binds to the side chains of the tetrahedral structure through base complementation. As an electroactive substance, MB could penetrate the groove of the nucleic acid double strand. Upon the addition of CAP, Apt-CAP would bind more tightly to the target CAP, and the associated conformational change could force it to be released from the tetrahedral structure, thereby causing MB that embedded in the double strand to be released to result in a decrease of the electrical signal in the PBS solution. Therefore, the CAP level could be quantified through determination of the peak current change of MB.

3.4 Characterization of AuNPs/rGO modified composite electrode

CV was used to verify the modification process of the glassy carbon electrode (Fig. S1A). Based on the uninterrupted redox reaction between Fe^{3+} and Fe^{2+}, the electrochemical response of $K_3[Fe(CN)_6]$ is reversible, producing a set of symmetrical redox peaks in the CV manner. At a scan rate of 50 mV/s, the peak spacing of bare GCEs is 69 mV (Fig. S1A, line a). After removing the oxygen-containing functional groups of graphene oxide by electroreduction, the peak current value increased significantly (Fig. S1A, line b), indicating that its electrical conductivity was increased, and the modified layer accelerated the electron transfer effect on the electrode surface. Meanwhile, the rGO modified by electrochemical reduction on the surface of GCE exhibited a yarn-like irregular wrinkle shape (Fig. S1B), which was consistent with the study by Qiu et al.[25].

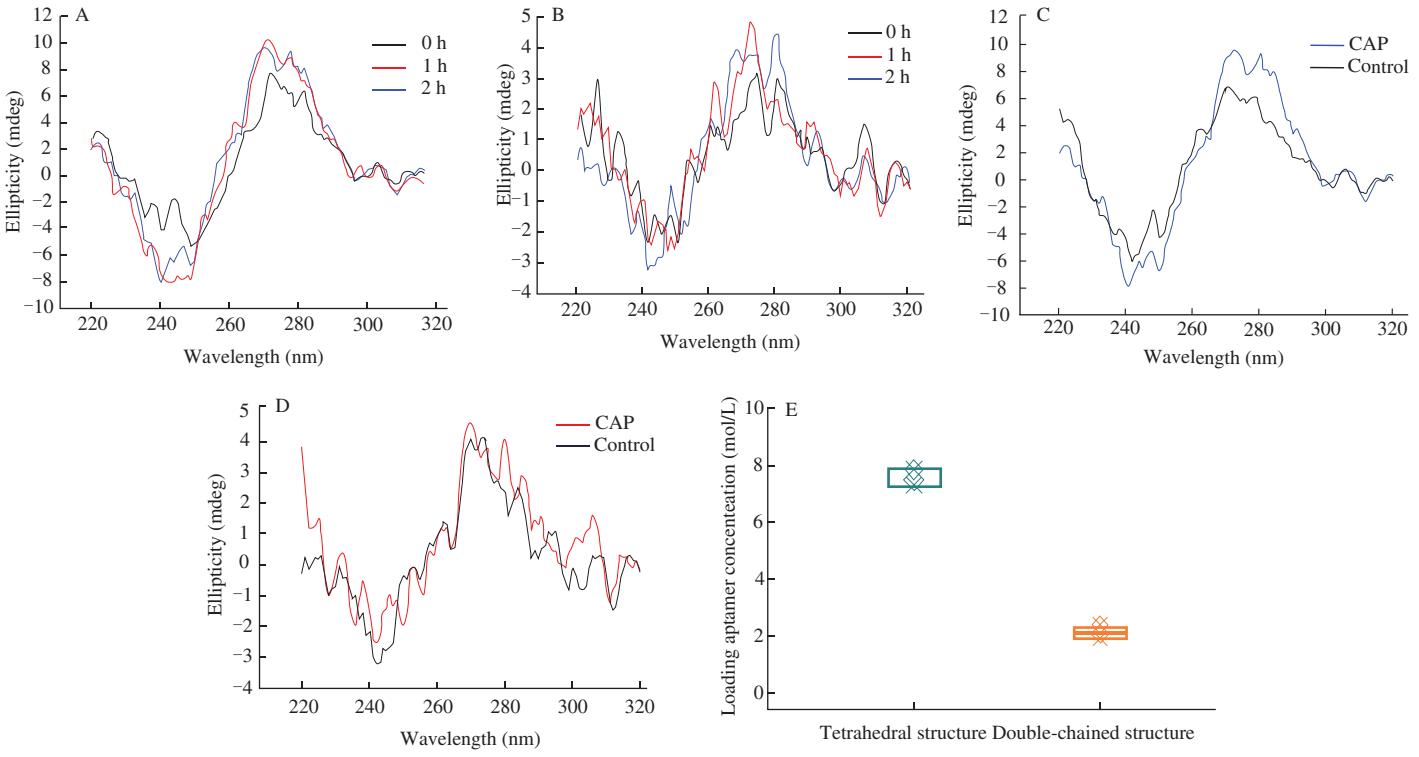

Fig. 2 Evaluation of superiority of tetrahedral structure to traditional double-chained structure for developing aptasensor. Conformational changes of (A) tetrahedral structure and (B) double-chained structure secondary to different placement time. CAP binding associated conformational changes of tetrahedral (C) structure and (D) double-chained structure. (E) Comparison of Apt-CAP loading capacity between tetrahedral structure and double-chained structure.

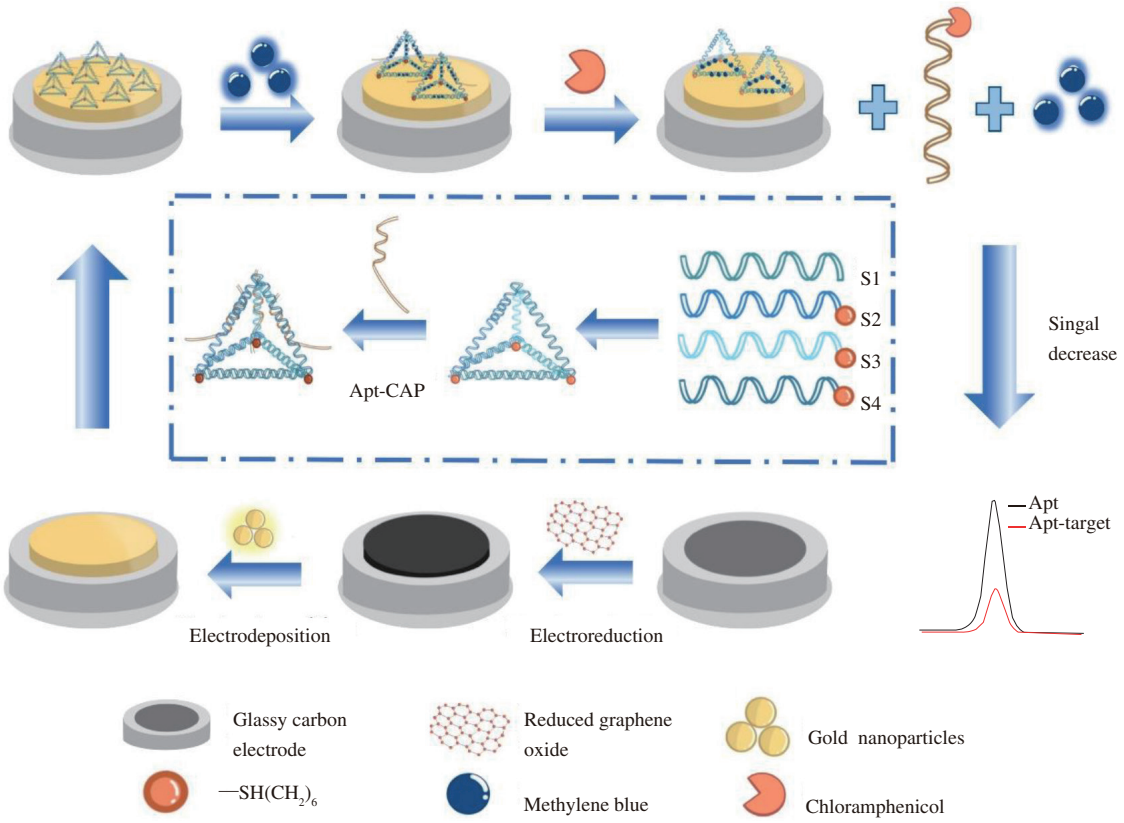

Fig. 3 Schematic illustration of the principle of the DNA tetrahedral structure-based electrochemical aptasensor.

Such shape could not only increase the electrode surface area which was confirmed by the increased peak current value (Fig. S1A, line b), but also provide more activity sites for the attachment of AuNPs[26]. After immobilization of AuNPs on the rGO/GCE, the peak current increased continuously (Fig. S1A, line c), indicating the good electrocatalytic activity of AuNPs to accelerate the electron transfer rate. Scanning electron microscope (SEM) image suggested that gold nanoparticles were aggregated on the surface of rGO/GCE and the average size was below 50 nm (Fig. S1C). Such structure could significantly increase the electrode surface to volume ratio to facilitate the transfer of electrons on the electrode surface[27], contributing to the increase of peak current value (Fig. S1A, line c).

After respective immobilization of the tetrahedra and tetrahedron-aptamer complex on the AuNPs/rGO/GCE electrode and blocking with MCH, the current showed a gradual decreasing tendency (Fig. S1A, lines d and e), which was due to the blocking of partial active sites on the electrode, inhibiting the mass transfer process of the negative charges of $[Fe(CN)_6]^{4-}$ and $[Fe(CN)_6]^{3-}$ on the electrode[28].

3.5 Optimization of the established electrochemical aptasenso

In this study, an electrochemical aptasensor targeting CAP was constructed based on the above detection principle, and the relevant factors affecting the detection efficiency of the aptasensor (loading tetrahedron concentration, incubation time of the tetrahedron-aptamer complex with the electrode and reaction time with the target CAP) were also optimized. According to the results, the optimal detection conditions for the fabricated aptasensor were as follows: a tetrahedral concentration of 2 μmol/L (Fig. 4A), 12 h incubation time to immobilize tetrahedron-aptamer complex on the electrode (Fig. 4B), and the final detection duration time of 30 min (Fig. 4C).

3.6 Analytical performance of the constructed targeted CAP aptasensor

The constructed aptasensor was used to detect different concentrations of CAP with optimized parameters. The logarithm of the CAP concentration (X) was linearly related to the ΔμA (Y) in the range of 0.6 nmol/L–1.2 μmol/L (0.19–387.76 ng/mL) (Fig. 5A). Meanwhile, the LOD of CAP for this aptasensor was determined to be 0.067 6 ng/mL (0.209 3 nmol/L). Such linear range and LOD value suggested improvement for detecting CAP in comparison to previous detection results revealed by standard methods GC analysis (LOD value of 0.07 μg/kg)[5], HPLC-MS analysis (LOD value of 2.69 μg/kg)[6], and enzyme-linked immunosorbent assay (LOD value of 10 ng/mL)[7]. Meanwhile, such linear range and LOD value presented here were also superior to previous reported aptamer-based sensors for detecting CAP. For example, Pilehvar et al.[29] and Alibolandi et al.[30] reported LOD values of 0.517 and 0.319 ng/mL, respectively, for detection of CAP. Moreover, our previous work also reported an aptasensor for detecting CAP with a LOD of 0.1 ng/mL (linear range of 0.1–20.0 ng/mL)[31]. The improved LOD value and linear range of this aptasensor suggested its application potential for effective detection of CAP residues.

The ΔμA value presented by this aptasensor for CAP was significantly higher than those for structural analogs of CAP (thiamphenicol, florfenicol and streptomycin) and the negative control (Fig. 5B),

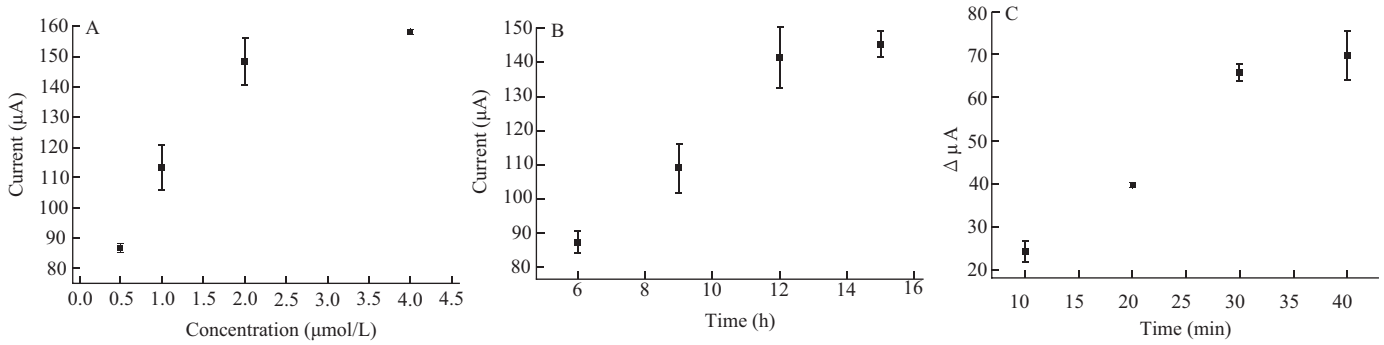

Fig. 4 Influence of the key experimental factors on the electrochemical aptasensor. (A) Loading tetrahedron concentration. (B) Incubation time of the tetrahedron-aptamer complex with the electrode. (C) Reaction time with the target CAP. The error bars are defined by the standard deviation of the results from 3 parallel experiments.

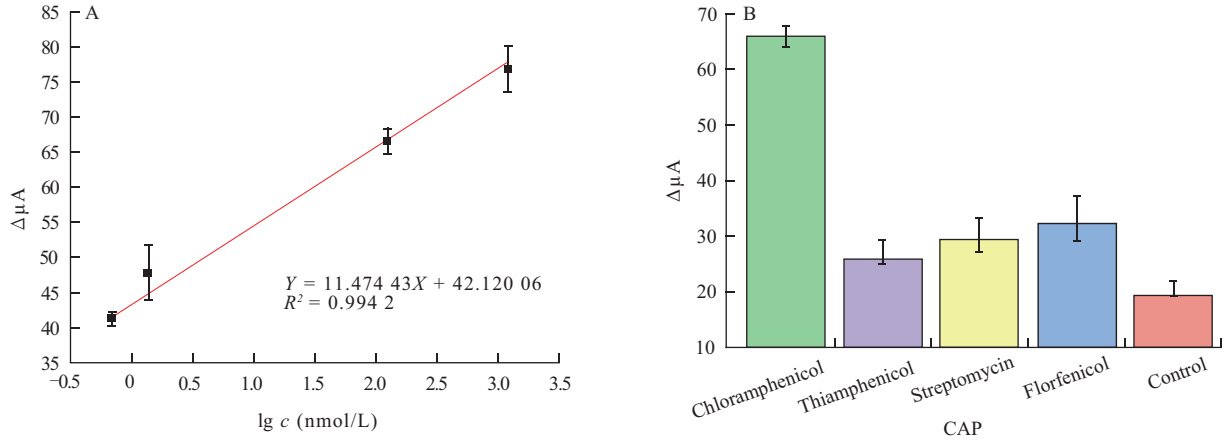

Fig. 5 Analytical performance of the constructed aptasensor for CAP detection. (A) The linearity of the peak current response of the electrochemical aptasensor with different concentrations of CAP. (B) The specificity of the aptasensor for CAP and its structural analogs (hiamphenicol, florfenicol, and streptomycin). The error bars are defined by the standard deviation of the results from 3 parallel experiments.

thereby reiterating high specificity of this aptasensor for detecting CAP. Moreover, good detection repeatability with 97.64% secondary detection efficiency (Fig. S2) and excellent detection stability (Table S2) further suggested the application potential of this aptasensor.

3.7 Application of the developed aptasensor to detect CAP in actual milk samples

To evaluate the application feasibility of the aptasensor, different CAP concentrations (5, 10 and 15 ng/mL) were spiked to actual milk samples, and the recovery rates of CAP were calculated as 101.69%, 100.57% and 101.30%, respectively (Table 1), illustrating that the aptasensor could be feasible for detection of CAP in real samples. Moreover, according to the market prices of chemicals and reagents used in this work, an amount of USD 1.34 per sample (Table S3) also confirmed the cost-effectiveness of the aptasensor.

4. Conclusion

In summary, results presented here suggested the superiority of tetrahedral structure to traditional double-chained structure for developing aptasensor. Then, a self-assembled DNA tetrahedral structure-based aptasensor with high sensitivity and specificity for detecting CAP was developed. Under the optimal conditions, the aptasensor exhibited high sensitivity toward CAP with a LOD of 0.067 6 ng/mL (linear range from 0.19 to 387.76 ng/mL) and high selectivity against structural analogs of CAP. Moreover, this aptasensor also suggested cost effective with detection cost of only USD 1.34 per sample and good reusability. Finally, good recovery rate of CAP from spiked milk samples further confirmed the application potential of this tetrahedral structure-based aptasensor for detecting CAP in animal-sourced food.

Table 1
Recovery rates for added CAP detection in spiked milk samples using the established aptasensor (n = 3).

Milk sample	Spiked CAP (ng/mL)	Measurement of CAP (mean ± SD, ng/mL)	Recovery rate (%)	RSD
No. 1	5	5.084 3 ± 0.325 9	101.69	0.067 1
No.2	10	10.057 2 ± 0.138 6	100.57	0.013 8
No.3	15	15.194 7 ± 1.105 5	101.30	0.072 8

Note: The mean is the mean of 3 experiments, SD is standard deviation and RSD is relative standard deviation.

Conflict of interest

The authors declare no conflicts of interest.

Acknowledgements

This work was supported by the National Nature Science Foundation of China (82174531) and the Medicine and Health Science Technology Development Project of Shandong Province, China (202212060626).

Appendix A. Supplementary data

Supplementary data associated with this article can be found, in the online version, at http://doi.org/10.26599/FSHW.2024.9250341.

References

[1] P. Moudgil, J.S. Bedi, R.S. Aulakh, et al., Validation of HPLC multi-residue method for determination of fluoroquinolones, tetracycline, sulphonamides and chloramphenicol residues in bovine milk, Food Anal. Method. 12 (2018) 338-346. https://doi.org/10.1007/s12161-018-1365-0.

[2] H. Kikuchi, T. Sakai, R. Teshima, et al., Total determination of chloramphenicol residues in foods by liquid chromatography-tandem mass spectrometry, Food Chem. 230 (2017) 589-593. http://doi.org/10.1016/j.foodchem.2017.03.071.

[3] J. Wongtavatchai, L. McLean, F. Ramos, et al., World health organization: joint FAO/WHO expert committee on food additives (JECFA), chloramphenicol, IPCS (international programme on chemical safety) INCHEM WHO Food Additives Series, 53 (2004) 7-85.

[4] Commission Regulation, Commission Regulation (EU) No 37/2010 of 22 December 2009 on pharmacologically active substances and their classification regarding maximum residue limits in foodstuffs of animal origin, The Official Journal of the European Communities, 2010, No. L 15/1-72.

[5] V. Cerkvenik-Flajs, Performance characteristics of an analytical procedure for determining chloramphenicol residues in muscle tissue by gas chromatography-electron capture detection, Biomed. Chromatogr. 20(10) (2006) 985-992. http://doi.org/10.1002/bmc.599.

[6] B. Er Demirhan, B. Demirhan, Detection of antibiotic residues in blossom honeys from different regions in Turkey by LC-MS/MS method, Antibiotics 11(3) (2022) 357. http://doi.org/10.3390/antibiotics11030357.

[7] N.A. Byzova, E.A. Zvereva, A.V. Zherdev, et al., Rapid pretreatment-free immunochromatographic assay of chloramphenicol in milk, Talanta 81(3) (2010) 843-848. http://doi.org/10.1016/j.talanta.2010.01.025.

[8] M. Zhao, X. Li, Y. Zhang, et al., Rapid quantitative detection of chloramphenicol in milk by microfluidic immunoassay, Food Chem. 339 (2021) 127857. http://doi.org/10.1016/j.foodchem.2020.127857.

[9] C. Acquah, D. Agyei, E.M. Obeng, et al., Aptamers: an emerging class of bioaffinity ligands in bioactive peptide applications, Crit. Rev. Food Sci. Nutr. 60(7) (2020) 1195-1206. http://doi.org/10.1080/10408398.2018.1564234.

[10] A. Chen, S. Yang, Replacing antibodies with aptamers in lateral flow immunoassay, Biosens. Bioelectron. 71 (2015) 230-242. http://doi.org/10.1016/j.bios.2015.04.041.

[11] M. Liu, A. Khan, Z. Wang, et al., Aptasensors for pesticide detection, Biosens. Bioelectron. 130 (2019) 174-184. http://doi.org/10.1016/j.bios.2019.01.006.

[12] L. Geng, H. Wang, M. Liu, et al., Research progress on preparation methods and sensing applications of molecularly imprinted polymer-aptamer dual recognition elements, Sci. Total Environ. 912 (2024) 168832. http://doi.org/10.1016/j.scitotenv.2023.168832.

[13] G.K. Mishra, V. Sharma, R.K. Mishra, Electrochemical aptasensors for food and environmental safeguarding: a review, Biosensors 8(2) (2018) 28. http://doi.org/10.3390/bios8020028.

[14] A. Díaz-Fernández, R. Lorenzo-Gómez, R. Miranda-Castro, et al., Electrochemical aptasensors for cancer diagnosis in biological fluids-a review, Anal. Chim. Acta 1124 (2020) 1-19. http://doi.org/10.1016/j.aca.2020.04.022.

[15] Z. Khoshbin, A. Verdian, M.R. Housaindokht, et al., Aptasensors as the future of antibiotics test kits-a case study of the aptamer application in the chloramphenicol detection, Biosens. Bioelectron. 122 (2018) 263-283. http://doi.org/10.1016/j.bios.2018.09.060.

[16] L. Geng, J. Sun, M. Liu, et al., Molecularly imprinted polymers-aptamer electrochemical sensor based on dual recognition strategy for high sensitivity detection of chloramphenicol, Food Chem. 437(Pt2) (2024) 137933. http://doi.org/10.1016/j.foodchem.2023.137933.

[17] Z. Gao, X. Du, Y. Ding, et al., Establishment of a dual-aptasensor for simultaneous detection of chloramphenicol and kanamycin, Food Addit. Contam. Part A-Chem. Anal. Control Expo. Risk Assess. 38(7) (2021) 1148-1156. http://doi.org/10.1080/19440049.2021.1914871.

[18] R.P. Goodman, R.M. Berry, A.J. Turberfield, The single-step synthesis of a DNA tetrahedron, Chem. Commun. 12 (2004) 1372-1373. http://doi.org/10.1039/b402293a.

[19] Y. He, T. Ye, M. Su, et al., Hierarchical self-assembly of DNA into symmetric supramolecular polyhedral, Nature 452(7184) (2008) 198-201. http://doi.org/10.1038/nature06597.

[20] X. Hui, C. Yang, D. Li, et al., Infrared plasmonic biosensor with tetrahedral DNA nanostructure as carriers for label-free and ultrasensitive detection of miR-155, Adv. Sci. 8(16) (2021) e2100583. http://doi.org/10.1002/advs.202100583.

[21] Y. Guo, F. Yang, Y. Yao, et al., Novel Au-tetrahedral aptamer nanostructure for the electrochemiluminescence detection of acetamiprid, J. Hazard. Mater. 401 (2021) 123794. http://doi.org/10.1016/j.jhazmat.2020.123794.

[22] J. Mehta, B. Van Dorst, E. Rouah-Martin, et al., *In vitro* selection and characterization of DNA aptamers recognizing chloramphenicol, J. Biotechnol. 155(4) (2011) 361-369. http://doi.org/10.1016/j.jbiotec.2011.06.043.

[23] S. Lee, K.M. Song, W. Jeon, et al., A highly sensitive aptasensor towards *Plasmodium* lactate dehydrogenase for the diagnosis of malaria, Biosens. Bioelectron. 35(1) (2012) 291-296. http://doi.org/10.1016/j.bios.2012.03.003.

[24] S. Liang, A.B. Kinghorn, M. Voliotis, et al., Measuring luteinising hormone pulsatility with a robotic aptamer-enabled electrochemical reader, Nat. Commun. 10(1) (2019) 852. http://doi.org/10.1038/s41467-019-08799-6.

[25] L. Qiu, X. Zhang, W. Yang, et al., Controllable corrugation of chemically converted graphene sheets in water and potential application for nanofiltration, Chem. Commun. 47(20) (2011) 5810-5812. http://doi.org/10.1039/c1cc10720h.

[26] C.Q. Wang, J. Du, H.W. Wang, et al., A facile electrochemical sensor based on reduced graphene oxide and Au nanoplates modified glassy carbon electrode for simultaneous detection of ascorbic acid, dopamine and uric acid, Sensor. Actuat. B-Chem. 204 (2015) 302-309. https://doi.org/10.1016/j.snb.2014.07.077.

[27] N. Huang, M. Liu, H. Li, et al., Synergetic signal amplification based on electrochemical reduced graphene oxide-ferrocene derivative hybrid and gold nanoparticles as an ultra-sensitive detection platform for bisphenol A, Anal. Chim. Acta 853 (2015) 249-257. http://doi.org/10.1016/j.aca.2014.10.016.

[28] M. Pourmadadi, J.S. Shayeh, M. Omidi, et al., A glassy carbon electrode modified with reduced graphene oxide and gold nanoparticles for electrochemical aptasensing of lipopolysaccharides from *Escherichia coli* bacteria, Mikrochim. Acta 186(12) (2019) 787. http://doi.org/10.1007/s00604-019-3957-9.

[29] S. Pilehvar, J. Mehta, F. Dardenne, et al., Aptasensing of chloramphenicol in the presence of its analogues: reaching the maximum residue limit, Anal. Chem. 84(15) (2012) 6753-6758. http://doi.org/10.1021/ac3012522.

[30] M. Alibolandi, F. Hadizadeh, F. Vajhedin, et al., Design and fabrication of an aptasensor for chloramphenicol based on energy transfer of CdTe quantum dots to graphene oxide sheet, Mater. Sci. Eng. C-Mater. Biol. Appl. 48 (2015) 611-619. http://doi.org/10.1016/j.msec.2014.12.052.

[31] Y. Duan, L. Wang, Z. Gao, et al., An aptamer-based effective method for highly sensitive detection of chloramphenicol residues in animal-sourced food using real-time fluorescent quantitative PCR, Talanta 165 (2016) 671-676. http://doi.org/10.1016/j.talanta.2016.12.090.